

By exploring glucocorticoid signaling, which does not affect the central circadian pacemaker in the SCN, we have determined that peripheral oscillators can be phase delayed or phase advanced during the entire 24-hour day. This phase-shifting behavior would be expected for slave oscillators that are synchronized by a master pacemaker because they should remain responsive to phase-resetting signals from the SCN at all times.

References and Notes

1. J. C. Dunlap, *Cell* **96**, 271 (1999).
2. S. A. Brown and U. Schibler, *Curr. Opin. Genet. Dev.* **9**, 588 (1999).
3. M. H. Hastings, *Curr. Biol.* **7**, 670 (1997).
4. B. Rusak and I. Zucker, *Physiol. Rev.* **59**, 449 (1979).
5. J. Blau and M. W. Young, *Cell* **99**, 661 (1999).
6. P. L. Lowrey et al., *Science* **288**, 483 (2000).
7. I. F. Emery, J. M. Noveral, C. F. Jamison, K. K. Siwicki, *Proc. Natl. Acad. Sci. U.S.A.* **94**, 4092 (1997).
8. D. Whitmore, N. S. Foulkes, U. Strähle, P. Sassone-Corsi, *Nature Neurosci.* **1**, 701 (1998).
9. A. Balsalobre, F. Damiola, U. Schibler, *Cell* **93**, 929 (1998).
10. S. Yamazaki et al., *Science* **288**, 682 (2000).
11. P. Emery, W. V. So, M. Kaneko, J. C. Hall, M. Rosbash, *Cell* **95**, 669 (1998).
12. R. Stanewsky et al., *Cell* **95**, 681 (1998).
13. M. F. Ceriani et al., *Science* **285**, 553 (1999).
14. D. Whitmore, N. S. Foulkes, P. Sassone-Corsi, *Nature* **404**, 87 (2000).
15. F. Tronche, C. Kellendonk, H. M. Reichardt, G. Schütz, *Curr. Opin. Genet. Dev.* **8**, 532 (1998).
16. P. Rosenfeld, J. A. M. Van Eekelen, S. Levine, E. R. De Kloet, *Dev. Brain Res.* **42**, 119 (1988).
17. ———, *Cell. Mol. Neurobiol.* **13**, 295 (1993).
18. L. Lopez-Molina, F. Conquet, M. Dubois-Dauphin, U. Schibler, *EMBO J.* **16**, 6762 (1997).
19. Rat-1 cells were grown and frozen as described (9). The dexamethasone shock was done as described (9) but with 100 nM dexamethasone (10 mM in ethanol) (Brunschwig AG, Basel, Switzerland). In control petri dishes, 0.001% ethanol in Dulbecco's minimum essential medium (DMEM) with penicillin-streptomycin-glutamine was added.
20. A breeding colony of MORO mice (Swiss mice from RCC Ltd., Füllinsdorf, Switzerland) was established within our temperature-controlled (22° to 24°C) facility in Geneva. GR^{AlpCre} and their respective wild-type control mice were established and housed within a temperature-controlled (20° to 22°C) facility at the Deutsches Krebsforschungszentrum (Heidelberg, Germany). GR^{AlpCre} mice come from a mixed background (129-C57BL/6-FVB/N). All lighting cycles were 12 hours light: 12 hours dark. Male and female mice 8 to 24 weeks of age were used (a single sex was used within the same experiment). Animal care was in accordance with institutional guidelines.
21. Brain cutting, tissue fixation, and in-situ hybridization were performed as described in (18).
22. A. Balsalobre et al., data not shown.
23. Web fig. 1 is available at Science Online at www.sciencemag.org/feature/data/1053506.shl.
24. Injection of 2 mg per kg of body weight (2 mg/kg) of dexamethasone 21-phosphate (400 µg/ml in phosphate-buffered saline (PBS)) (D-1159, Sigma) or solvent (PBS with 0.15% ethanol) was performed intraperitoneally under red light (during the night) or under ambient light (during the day). Dexamethasone-phosphate was used instead of free-dexamethasone (as was used in the in vitro experiments) for solubility reasons. We also confirmed that dexamethasone 21-phosphate produced the same results as dexamethasone in vitro (22).
25. A phase shift is normally defined as a steady-state change in phase that is maintained during a subsequent free-run of the oscillator. The term apparent phase shift response curve (aPRC) was used here because only transient phase shifts could be recorded upon dexamethasone injection. After one cycle, the SCN pacemaker re-established its dominance in the periphery.

26. S. Daan and C. S. Pittendrigh, *J. Comp. Physiol.* **106**, 253 (1976).
27. C. Kellendonk, C. Opherk, K. Anlag, G. Schütz, F. Tronche, *Genesis* **26**, 151 (2000).
28. N. Le Minh, F. Damiola, F. Tronche, C. Kellendonk, G. Schütz, U. Schibler, unpublished data.

29. Supported by the Swiss National Science Foundation, the Louis-jeantet Foundation for Medicine, and the State of Geneva (U.S.) and by the Deutsche Forschungsgemeinschaft and the European Union (G.S.).

26 June 2000; accepted 11 August 2000

Dendritic Computation of Direction Selectivity by Retinal Ganglion Cells

W. Rowland Taylor,^{1,2*} Shigang He,⁴ William R. Levick,^{2,3} David I. Vaney⁴

Direction-selective ganglion cells (DSGCs) in the retina respond strongly when stimulated by image motion in a preferred direction but are only weakly excited by image motion in the opposite null direction. Such coding represents an early manifestation of complex information processing in the visual system, but the cellular locus and the synaptic mechanisms have yet to be elucidated. We recorded the synaptic activity of DSGCs using strategies to observe the asymmetric inhibitory inputs that underlie the generation of direction selectivity. The critical nonlinear interactions between the excitatory and inhibitory inputs took place postsynaptically within the dendrites of the DSGCs.

In the vertebrate visual system, the encoding of the direction of image motion first occurs in specialized types of retinal ganglion cells, within two or three synapses of the photoreceptor input. These DSGCs have been most extensively studied in the rabbit retina, where two distinct types of DSGCs respond either at the onset and termination of a light stimulus (On-Off DSGCs) or only at the onset of a light stimulus (On DSGCs) (1, 2). The more commonly encountered On-Off DSGCs comprise four physiological subtypes, whose preferred directions are aligned with the horizontal and vertical ocular axes (3).

Extracellular recordings indicate that the key mechanism underlying direction selectivity in DSGCs is spatially asymmetric inhibition, which counteracts excitation for motion in the null direction but not in the preferred direction (2, 4, 5). Pharmacological studies show that γ -aminobutyric acid (GABA) antagonists abolish the direction selectivity of DSGCs, indicating that a GABAergic input from lateral association neurons (amacrine cells) inhibits the excitatory inputs arising from the glutamatergic second-order interneurons (bipolar cells) and from cholinergic amacrine cells (6–8). These studies leave a fundamental question

unanswered: Where do the inhibition and excitation interact? The null-direction inhibition might act presynaptically on the excitatory inputs to the DSGC (Fig. 1, upper panels), in which case the release of transmitter from the excitatory neuron would itself be direction selective. Alternatively, the null-direction inhibition might act postsynaptically on the ganglion cell dendrites (Fig. 1, lower panels) by shunting the excitatory currents through an inhibitory chloride conductance with a reversal potential near the resting potential (shunting inhibition) (7, 9, 10).

Patch-clamp recordings (11) revealed that the On-Off DSGCs generate excitatory postsynaptic potentials (EPSPs) to the leading edge (On response) and trailing edge (Off response) of a light bar moving in any direction through the receptive field, but stimuli moving in the preferred direction produced stronger excitation than stimuli moving in the null direction or in orthogonal directions (Fig. 2A). We measured the On and Off responses to eight directions of motion (12), in terms of both the amplitude of the EPSPs and the number of spikes produced, then plotted the responses in polar coordinates. When the eight individual response vectors are summed, the direction of the resultant vector indicates the preferred direction. This was always similar for the On and Off responses. The length of the resultant vector gives an indication of the strength of the direction selectivity and will tend toward zero for direction-independent responses. EPSPs were elicited by movements in all directions, whereas

¹John Curtin School of Medical Research, ²Centre for Visual Sciences, ³Department of Psychology, Australian National University, Canberra, ACT 2601, Australia. ⁴Vision, Touch and Hearing Research Centre, School of Biomedical Sciences, University of Queensland, Brisbane, QLD 4072, Australia.

*To whom correspondence should be addressed. E-mail: Rowland.Taylor@anu.edu.au

spikes occurred only for directions close to the preferred direction, thus confirming that the spike threshold serves to sharpen the direction selectivity (Fig. 2, B and C). The relative amplitudes of the EPSPs in the preferred and null directions were unchanged when the spiking activity was abolished with sodium-channel blockers

applied either intracellularly [10 mM QX-314 (Sigma)] or extracellularly [0.5 μ M tetrodotoxin (Sigma)]. These results indicate that the generation of direction selectivity is not contingent on voltage-dependent conductances in either the DSGC or the presynaptic interneurons.

Depolarizing the membrane potential of

the DSGC will change the balance between inhibitory and excitatory currents by reducing the driving force of the excitation and increasing the driving force of the inhibition (13). If the null-direction inhibition acts directly on the DSGC, depolarization will differentially affect the responses to preferred- and null-direction motions, which will be quantitatively reflected by an increase in the length of the resultant vector. (The resultant vector would be unaffected by symmetrical surround inhibition because nondirectional components will cancel when the individual response vectors are summed.) If the null-direction inhibition acts presynaptically, depolarization will proportionally reduce both the strong excitation produced by preferred-direction motion and the weak excitation produced by null-direction motion, thus reducing the length of the resultant vector.

We voltage-clamped DSGCs at -70 and -30 mV and recorded the synaptic currents elicited by a light bar moving through the receptive field in eight directions. When the cell was depolarized, the differences in the synaptic currents elicited by preferred- and null-direction motions became more pronounced; this is reflected in the stronger asymmetry of the polar plots at -30 mV (Fig. 3). In quantitative terms, the length of the resultant vector increased 2.4 ± 2.0 times ($n = 8$), despite an overall decrease in the absolute amplitudes of the synaptically evoked currents. This supports the hypothesis that a major component of the direction selectivity is generated by null-

Fig. 1. Presynaptic and postsynaptic models of direction selectivity. P, photoreceptor; BC, bipolar cell; AC, amacrine cell; GC, direction-selective ganglion cell. Direction selectivity is generated by the nonlinear interaction of vertically transmitted excitation and spatially offset inhibition, presumed to arise from a type of GABAergic amacrine cell. The inhibition could impinge either presynaptically on the terminals of the excitatory interneurons (upper panels) or postsynaptically on the dendrites of the ganglion cell (lower panels). For image motion in the null direction, the firing of the ganglion cell is suppressed by the spatial and temporal coincidence of inhibition and excitation (gray spots); for image motion in the preferred direction, excitation and inhibition are temporally but not spatially coincident and the cell fires.

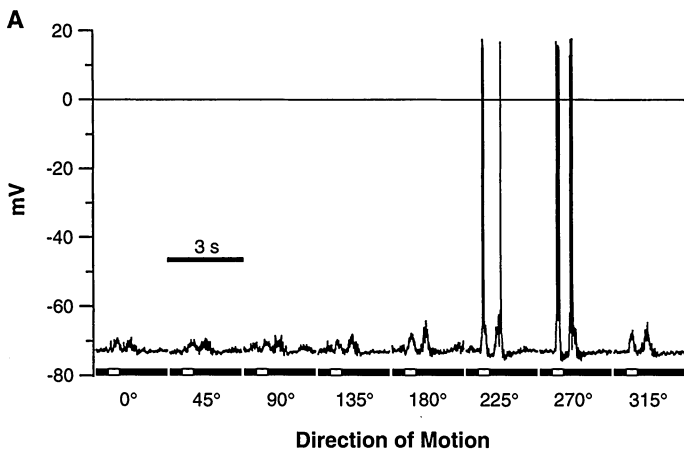
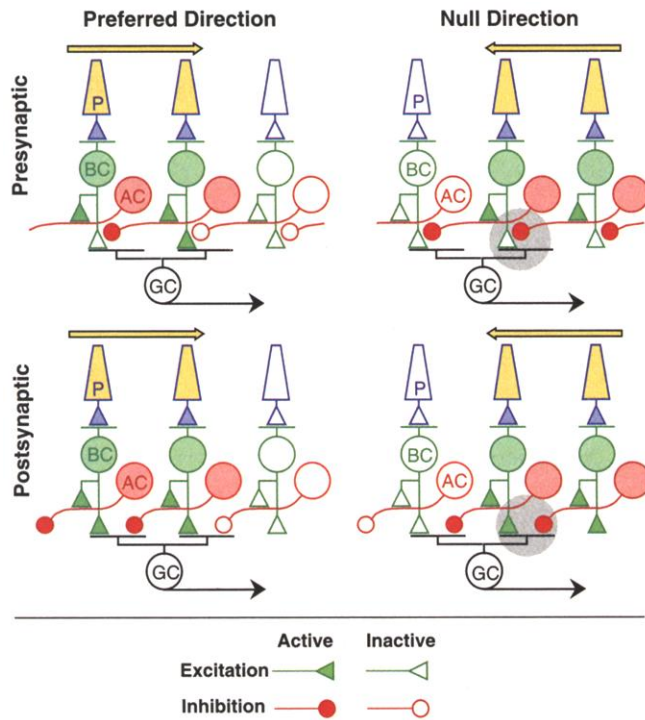
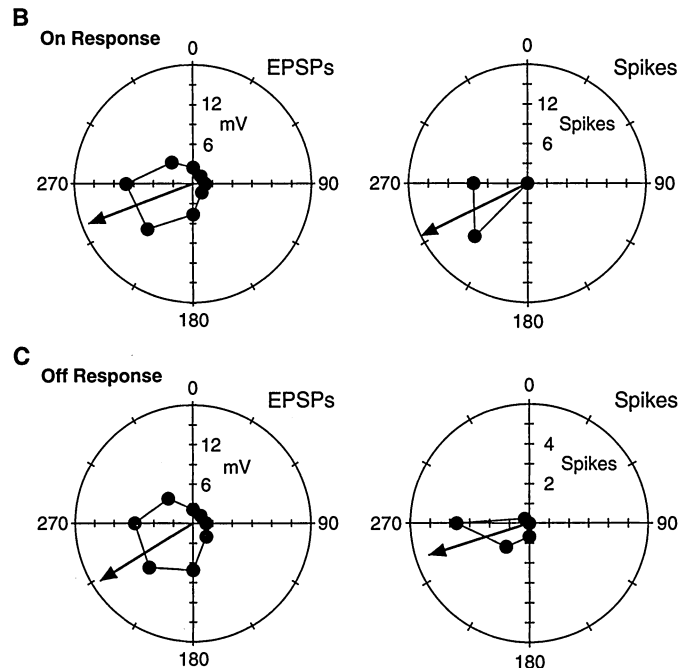


Fig. 2. Direction selectivity in a retinal ganglion cell. (A) Intracellular responses elicited by a light bar moving through the center of the receptive field; the direction of image motion is shown beneath the records. An On EPSP was generated by the dark-to-light transition at the leading edge of the stimulus, and an Off EPSP was generated by the light-to-dark transition at the trailing edge. For motion close to the preferred direction ($\sim 250^\circ$), the EPSPs elicited a burst of spikes. (B and C) Polar plots of the On responses and Off responses, respectively, where the angle represents the motion direction, and the radius represents the response amplitude. The peak amplitudes of the evoked EPSPs are plotted in the left-hand panels, and the numbers of elicited spikes are plotted in the right-hand panels (average of six individual responses). The arrow in each panel represents the vector sum of the responses to the eight directions of motion.



REPORTS

direction inhibition acting postsynaptically on the ganglion cell dendrites.

If the asymmetric inhibition is mediated by GABA-activated chloride channels on the ganglion cell dendrites, then the direction selectivity should disappear in recordings made with high intracellular chloride concentrations. This will shift the chloride equilibrium (reversal) potential toward 0 mV, at which point both inhibitory and excitatory inputs will produce inward currents. When a 130 mM Cl⁻ patch solution was used (14), the cell initially displayed

strong directional responses at -30 mV (Fig. 4A), but as chloride diffused into the cell, the outward currents disappeared, and the direction of stimulus motion could no longer be discerned from the waveform of the responses (Fig. 4B). Similar results were obtained in five cells. These effects occurred within 1 to 5 min of breaking into the cell, whereas cells recorded with normal solutions (10 mM Cl⁻) retained their direction selectivity for at least 10 min (Fig. 4, C and D) and often for much longer. Given that the combined inward

currents produced by inhibitory and excitatory inputs under high chloride conditions are directionally symmetric, this is compatible with the parsimonious hypothesis that either input, if measured in isolation, would also be directionally symmetric. With such a model, the asymmetry in the responsiveness of the DSGC arises because the excitation is temporally coincident with the spatially offset inhibition for motion in the null direction but not in the preferred direction.

Because direction selectivity is generat-

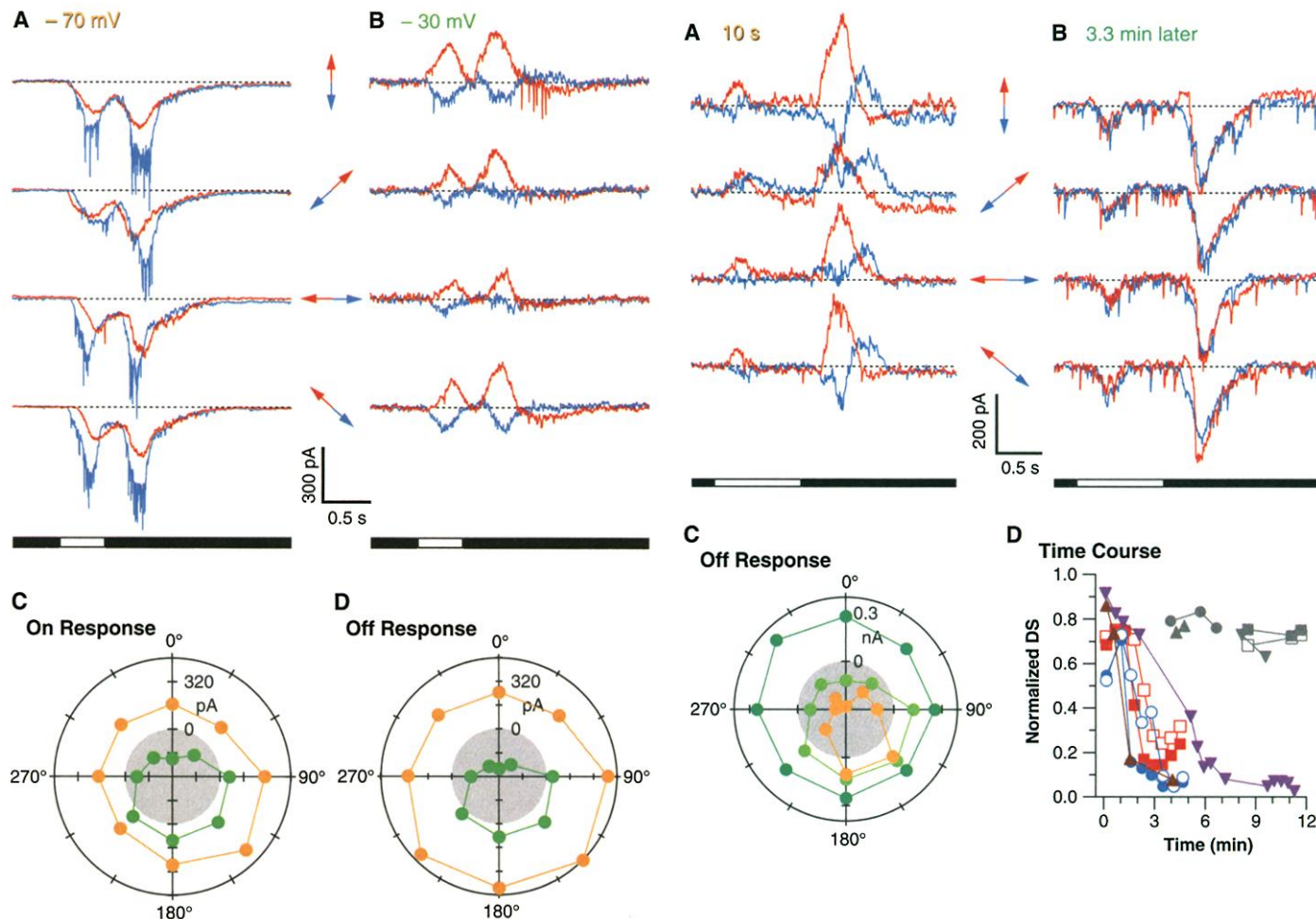


Fig. 3 (left). Depolarization increases directional asymmetry. (A and B) Net synaptic currents elicited in a DSGC by image motion in eight directions, indicated by the corresponding colored arrows; each record is the average of five (A) or three (B) individual responses. Compared with preferred direction responses (blue traces), motion directions with a null-direction component (red traces) produced slightly smaller inward currents at a holding potential of -70 mV (A) and net outward currents at -30 mV (B). (C and D) Polar plots of the data presented in (A) and (B) (yellow symbols, -70 mV; green symbols, -30 mV) (-320 pA at center). Under voltage clamp, inward (negative) currents are excitatory and are plotted as positive values on the polar plots; conversely, outward (positive) currents are inhibitory and are plotted as negative values. Responses with net inhibitory amplitudes fall within the central gray region, the circumference of which marks the zero current level. With this sign convention, the polar plots are asymmetric toward the preferred direction. **Fig. 4 (right).** High intracellular chloride concentrations reduce direction selectivity. (A and B) Net synaptic currents elicited in a DSGC by image motion in eight directions are indicated by the corresponding

colored arrows. Upon establishing the whole-cell configuration (clamped at -30 mV), motion directions with a null-direction component produced net outward currents (A), but as the high chloride concentration in the recording solution diffused into the cell, the direction selectivity of the responses was abolished (B). (C) Polar plot of the Off responses at times of 10 s (yellow), 1.0 min (light green), and 3.3 min (dark green), showing the rapid breakdown in direction selectivity; the sign convention is similar to Fig. 3, C and D, with the gray region delineating net inhibitory responses. (D) During equilibration with high intracellular chloride concentrations, the normalized direction selectivity of four DSGCs declined to low levels for both the On responses (open colored symbols) and the Off responses (solid colored symbols); four other DSGCs recorded at -30 mV with a normal recording solution showed no decline in direction selectivity with time (gray symbols). (The normalized direction selectivity was calculated by dividing the length of the vector sum by the summed lengths of the component vectors. This index varies from 0 for direction-independent responses to 1 in the case where the cell responds to only one direction of motion.)

ed locally within the receptive field of a DSGC (2), the asymmetric inhibitory inputs must affect only a local region ("sub-unit") of the dendritic tree. This is consistent with the postsynaptic inhibition being of a shunting, and thus divisive, nature (15). Moreover, the dendritic architecture of the DSGCs appears to provide an appropriate substrate for such postsynaptic interactions. In both the On and Off sublaminae of the inner plexiform layer, dendrites of all orders give rise to thin terminal branches, which cover the dendritic field in a space-filling lattice (16, 17). These terminal dendrites provide sites away from the main dendritic trunks where excitatory and inhibitory inputs may interact locally. Nevertheless, postsynaptic inhibition could produce a distinct asymmetry between the preferred and null sides of the receptive field. When a null-direction stimulus enters the null side of the dendritic field, much of the inhibition impinges proximally, between the excitatory inputs and the cell body. When the stimulus crosses to the preferred side, much of the inhibition impinges more distally to the excitatory inputs and may extend beyond the edge of the dendritic field. Thus, a functional asymmetry may arise because modeling studies predict that an inhibitory shunt located proximally to the excitatory input is much more effective than a similar input located distally (10). This arrangement might produce aberrant responses to some moving stimuli and may explain the presence of a nondirectional zone on the preferred side of DSGCs, covering as much as 20 to 25% of the receptive field (2, 18).

Our study demonstrates a major role for postsynaptic dendritic processing in a clearly defined and well-characterized neuronal computation, thus providing strong support for the theoretical studies that advocated such interactions (9, 10, 15). Many questions about the cellular mechanism of direction selectivity in the retina remain to be answered (5); the most important ones concern the identity of the GABAergic amacrine cells that mediate the null-direction inhibition and the manner in which they selectively contact different subtypes of DSGCs with different preferred directions. The results of this study, showing that the null-direction inhibition acts directly on the ganglion cell dendrites, provide a critical guidepost for future investigations.

References and Notes

1. H. B. Barlow, R. M. Hill, W. R. Levick, *J. Physiol.* **173**, 377 (1964).
2. H. B. Barlow and W. R. Levick, *J. Physiol.* **178**, 477 (1965).
3. C. W. Oyster and H. B. Barlow, *Science* **155**, 841 (1967).
4. F. R. Amthor and N. M. Grzywacz, *J. Neurophysiol.* **69**, 2174 (1993).
5. S. He and R. H. Masland, *Nature* **389**, 378 (1997).
6. H. J. Wyatt and N. D. Daw, *Science* **191**, 204 (1976).

7. M. Ariel and N. W. Daw, *J. Physiol.* **324**, 161 (1982).
8. C. A. Kittila and S. C. Massey, *J. Neurophysiol.* **77**, 675 (1997).
9. V. Torre and T. Poggio, *Proc. R. Soc. London Ser. B* **202**, 409 (1978).
10. C. Koch, T. Poggio, V. Torre, *Philos. Trans. R. Soc. London Ser. B* **298**, 227 (1982).
11. The techniques for making patch recordings from retinal ganglion cells followed those of Taylor and Wässle (19). Retinas from dark-adapted pigmented rabbits were isolated under infrared illumination (940 nm) and then flat-mounted with the photoreceptors down in a recording chamber on the fixed stage of an upright microscope. The preparation was continuously superfused (3 ml/min) with oxygenated Ames medium at 35° ± 0.2°C. On-Off DSGCs were initially targeted under infrared illumination as having a round medium-sized soma (~15 μm in diameter) with a crescent-shaped nucleus (17). The overlying inner limiting membrane and surrounding Müller cell end feet were microdissected away, and a patch electrode (3 to 7 megohms) was applied to the exposed soma. Membrane voltage or membrane current was recorded with an Axopatch 200B amplifier in the whole-cell recording configuration. Signals were filtered at 2 kHz (eight-pole Bessel filter) and sampled at 5 to 10 kHz.
12. Visual stimuli were generated on a Barco display monitor and projected onto the back focal plane of a ×40 (0.8 numerical aperture) water-immersion microscope objective, which focused the image onto the photoreceptor outer segments. The ×40 objective illuminated a region of retina with a diameter of ~500 μm. The stimulus consisted of a light bar, which was 250 μm wide and at least 500 μm long, moving across the stimulus region at 1 mm/s on a trajectory parallel to the long axis. The length of the bar ensured that the leading and trailing edges did not appear within the stimulus region simultaneously, thus allowing for adequate separation of the leading-edge (On) and trailing-edge (Off) responses. In Figs. 2A; 3, A and B; and 4, A and B, the stimulus timing is shown by a light bar beneath the

records; the start and finish of the white bar mark the entry into the stimulus region of the leading and trailing edges, respectively.

13. P. L. Marchiafava, *Vision Res.* **19**, 1203 (1979).
14. The external solution was Ames medium, a bicarbonate-buffered physiological saline equilibrated to pH 7.45 with 95% O₂/5% CO₂ and containing a full complement of amino acids, vitamins, and glucose. The ionic composition of the external solution was as follows: 120 mM NaCl, 23 mM NaHCO₃, 3.1 mM KCl, 1.15 mM CaCl₂, and 1.2 mM MgCl₂. Recording electrodes were filled with a solution (pH 7.4) containing 120 mM K-gluconate, 5 mM NaCl, 5 mM KCl, 5 mM Hepes, 1 mM MgCl₂, 1 mM EGTA, 1 mM adenosine 5'-triphosphate, and 0.1 mM guanosine 5'-triphosphate. For the voltage-clamp recordings shown in Fig. 3, potassium was replaced with cesium. For the high-chloride experiments shown in Fig. 4, K-gluconate was replaced with CsCl. In order to work quickly to observe the changes resulting from chloride loading, the command potential for the voltage clamp was set to -30 mV before break-in, and recording commenced immediately upon rupture of the membrane beneath the recording electrode.
15. C. Koch, T. Poggio, V. Torre, *Proc. Natl. Acad. Sci. U.S.A.* **80**, 2799 (1983).
16. C. W. Oyster, F. R. Amthor, E. S. Takahashi, *Vision Res.* **33**, 579 (1993).
17. D. I. Vaney, *J. Neurosci.* **14**, 6301 (1994).
18. S. He, Z. F. Jin, R. H. Masland, *J. Neurosci.* **19**, 8049 (1999).
19. W. Taylor and H. Wässle, *Eur. J. Neurosci.* **7**, 2308 (1995).
20. This work was supported by a National Health and Medical Research Council project grant to D.I.V. and W.R.T. and through recurrent funding by the John Curtin School of Medical Research to W.R.T. We thank J. M. Bekkers, P. Sah, G. Stuart, and B. Walmsley for helpful comments on the manuscript.

14 April 2000; accepted 11 August 2000

Failure to Regulate TNF-Induced NF-κB and Cell Death Responses in A20-Deficient Mice

Eric G. Lee,* David L. Boone,* Sophia Chai, Shon L. Libby, Marcia Chien, James P. Lodolce, Averil Ma†

A20 is a cytoplasmic zinc finger protein that inhibits nuclear factor κB (NF-κB) activity and tumor necrosis factor (TNF)-mediated programmed cell death (PCD). TNF dramatically increases A20 messenger RNA expression in all tissues. Mice deficient for A20 develop severe inflammation and cachexia, are hypersensitive to both lipopolysaccharide and TNF, and die prematurely. A20-deficient cells fail to terminate TNF-induced NF-κB responses. These cells are also more susceptible than control cells to undergo TNF-mediated PCD. Thus, A20 is critical for limiting inflammation by terminating TNF-induced NF-κB responses *in vivo*.

During inflammatory responses, TNF and interleukin-1 (IL-1) signals activate NF-κB, which regulates the transcription of other proinflammatory genes. The factors that limit

these responses are poorly understood. A20 is a cytoplasmic protein thought to be expressed predominantly in lymphoid tissues, and heterologously expressed A20 can inhibit TNF-induced NF-κB and PCD responses in cell lines (1-4). A20 binding to TNF receptor-associated factor-2 (TRAF2), inhibitor of NF-κB kinase gamma (IKKγ), and/or A20-binding inhibitor of NF-κB activation (ABIN) suggest potential mechanisms by which A20 could regulate TNF receptor signals (5-7);

Department of Medicine, The University of Chicago, 5841 South Maryland Avenue, MC 6084, Chicago, IL 60637, USA.

*These authors contributed equally to this work.
†To whom correspondence should be addressed. E-mail: ama@medicine.bsd.uchicago.edu